Supporting Information

Robinson et al. 10.1073/pnas.1215241109

SI Materials and Methods

Protein Purification. ***Native Mediator Head module.*** For preparation of the native Mediator Head complex *Saccharomyces cerevisiae* harboring Med8-TAP/ΔSin4 were grown in 200L YPAD to 9.0 A_{600} and 3.0 kg cells were lysed by continuous-flow bead beating in A25 buffer [25 mM ammonium sulfate, 100 mM Hepes pH 7.8, 1 mM EDTA, 5% (vol/vol) glycerol, 5 mM DTT, and 1× protease inhibitor mixture (0.6 μM leupeptin hemisulfate, 2 μM pepstatin A, 1 mM PMSF and 2.1 mM benzamidine hydrochloride)] with 25 μg/mL RNase A (Qiagen). The cell debris was pelleted by centrifugation at 12,250 × *g* for 1 h at 4 °C and the supernatant made up to 300 mM ammonium sulfate with the addition of cold 3.9 M ammonium sulfate and gentle stirring. Nucleic acids were depleted from the lysate by adding 500 mL DEAE (GE Healthcare) pre-equilibrated in A300 buffer. After 30 min of stirring the DEAE was pelleted by centrifugation (12,250 × *g*, 30 mins at 4 °C) and the supernatant loaded onto an IgG column before washing in A500 buffer. A mixture of Mediator Head and Head+Middle were eluted by tobacco etch virus (TEV) digestion directly onto a 5-mL HiTrap Q column (GE Healthcare) in Q50 buffer (50 mM ammonium sulfate, 50 mM Hepes pH 7.8, 5% vol/vol glycerol, 2 mM DTT) and the two complexes were resolved over a 50–600 mM ammonium sulfate gradient. The Head fractions were further purified by gel filtration on Sephacryl S400 (GE Healthcare).

In vitro transcription assay components. Full-length TBP was subcloned into pRSFDuet vector (Novagen) and overexpressed in Rosetta 2 (DE3) cells (Novagen). Overexpressed TBP was purified by Heparin and SP-Sepharose gradient chromatography. The TFIIA subunits ToaI and ToaII were independently subcloned into the pRSF vector (Novagen), overexpressed separately in Rosetta 2 (DE3) cells (Novagen), and purified from inclusion bodies under denaturing conditions. TFIIA was reconstituted by refolding purified ToaIp and ToaIIp as described previously (1). Full-length TFIIB with a His_6 N-terminal tag was purified as described previously (2). The TFIIE subunits Tfa1 (N-term His_6 tag) and Tfa2 were subcloned into MCS-I and -II of pRSFDuet and coexpressed in Rosetta 2 (DE3) cells. Overexpressed TFIIE was purified by Ni^{2+}-affinity (GE Healthcare), Mono-Q (Bio-Rad), and Superdex 75 (GE Healthcare) gel-filtration chromatography steps. The purification of wild-type and Kin28-AS TFIIH complexes from *S. cerevisiae* was performed identically; yeast cells grown to 9.0 A_{600} in YAPD were lysed in K400 buffer [400 mM KOAc, 50 mM Hepes pH 7.6, 1 mM EDTA, 5% (vol/vol) glycerol, 10 mM βME, 0.1% 3-(Decyldimethylammonio) propanesulphonate inner salt (3D-MAP) and 1× protease inhibitor mixture]. After clearing the cellular debris (12,250 × *g*, 60 min at 4 °C) the lysate was slowly brought to 100 mM ammonium sulfate (30 min) before the nucleic acid was precipitated with the addition of 0.2% wt/vol Polyethyleneimine (PEI) and removed by high-speed centriguation (12,250 × *g*, 60 min at 4 °C). The supernatant was loaded on an IgG column, which was then washed with 2 L K300 buffer before equilibration in cleavage buffer [300 mM KOAc, 50 mM Hepes pH 7.6, 5% (vol/vol) glycerol, 2 mM DTT, 0.1% 3D-MAP] and overnight TEV cleavage. Eluted TFIIH was further purified by 10–40% glycerol gradient fractionation (SW41Ti rotor for 25 h at 35 K rpm) in gradient buffer (10/40% glycerol vol/vol, 20 mM Hepes pH 7.6, 5 mM DTT, 0.1% 3D-MAP). Pol II-IIF was reconstituted from Pol II and TFIIF purified separately. To purify TFIIF, *S. cerevisiae* harboring C-terminally TAP-tagged Tfg2 grown to 9.0 A_{600} in YAPD were lysed in TEZ200 [200 mM ammonium sulfate, 50 mM Tris (pH7.5), 1 mM EDTA, 10 μM ZnCl2, 0.15% 3D-MAP, 3 mM DTT and 1× protease inhibitor mixture]. Following centriguation (12,250 × *g*, 60 min at 4 °C) the lysate was stirred with 0.25% PEI overnight, the nucleic acids pelleted (12,250 × *g*, 60 min at 4 °C), and supernatant loaded onto an IgG column. Bound TFIIF was washed with TEZ500, then and TEZ25, and was eluted in TEZ200 after overnight TEV cleavage. Eluted TFIIF was further purified by gradient fractionation on a 5 mL Heparin HiTrap column (GE Healthcare).

RNA Pol II and Mediator were purified simultaneously from a double-tagged yeast strain using an almost identical method to that described above for the Mediator Head module. The method only differs in the IgG cleavage steps, which involves two independent overnight incubations; Mediator is released from the resin by TEV cleavage within the N-terminal TAP tag of Med17 and PolII is released by 3C cleavage within the Protein G tag at the C terminus of Rpb1. All buffers and chromatography steps remain identical to the procedure described above.

To generate the Pol II-IIF complex, pure TFIIF and yeast Pol II were mixed at 1.6:1.0 molar ratio and dialyzed into buffer lacking detergent (150 mM KOAc, 10 mM Tris pH 7.5, 10 μM ZnCl2, 5% (vol/vol) glycerol, and 10 mM DTT) before the soluble complex was isolated by gel filtration using Superose 6 (GE Healthcare).

In Vitro Transcription Assays. For the fully reconstituted assay the promoter template was generated by first subcloning a 208-bp fragment comprising a 202-bp portion of the *S. cerevisiae HIS4* promoter (−104 to +98) flanked by EcoRV blunt ends into EcoRV-linearized pDrive vector (Qiagen). The 208-bp fragment with nonnative 6-bp flanking sequence was released from amplified vector with EcoRV digestion and purified by gel extraction from 2% agarose gels. In the transcription assay 5-pmol dsDNA template, 7.5 pmol TFIIB, 7.5 pmol TFIIA, 5 pmol TBP, 7.5 pmol TFIIE, 3 pmol wild-type or Kin28-AS TFIIH with or without 3 pmol Mediator were mixed in buffer A [300 mM KOAc, 50 mM Hepes pH 7.6, 5 mM DTT, and 5% (vol/vol) glycerol] and incubated at room temperature for 15 min. Next, 2 pmol RNA polII-IIF complex was added with or without NA-PP1 and the total volume made up to 14 μL with buffer B [30 mM KOAc, 50 mM Hepes pH 7.6, 5 mM DTT, and 5% (vol/vol) glycerol]. After a 15-min incubation at room temperature, transcription was initiated by adding 14 μL of buffer B containing 1.6 mM ATP, 1.6 mM GTP, 1.6 mM CTP, 40 μM UTP, 10 mM MgOAc, 1 unit RNaseOUT (Invitrogen) and 5 μCi [α -^{32}P]-UTP. The reaction mix was incubated for 45 min at 30 °C and stopped by adding 165 μL stop buffer (300 mM NaOAc pH 5.5, 10 mM Tris pH 8.0, 5 mM EDTA, 0.7% SDS, 0.1 mg/mL glycogen, and 0.013 mg/mL proteinase K) with a 15-min incubation at 37 °C. RNA was recovered by ethanol precipitation and analyzed with 10% denaturing PAGE and phosphoimaging, as described previously (3).

Assays in which promoter-specific carboxyl-terminal domain (CTD)-kinase activity was monitored alongside the corresponding transcription output were performed as described above, except for the following modifications: (*i*) 5 μCi [γ -^{32}P]-ATP was included in the reaction buffer, (*ii*) the reaction volume was doubled, and (*iii*) half of each reaction was stopped by transferring to an equal volume of 2× SDS gel loading buffer before 4–12% Bis-Tris PAGE (Invitrogen) and phosphoimage quantification.

Whole-cell extract (WCE) assays were performed with a plasmid template containing the yeast CYCJ promoter with GCN4 UAS (pGCN4:G-) essentially as described previously (4). Briefly, ~40 μg WCE [prepared as described previously (5)] with en-

dogenous Med7-TAP Mediator either present or depleted was preincubated with varying quantities of pure Mediator (±500 ng), Mediator Head (±2 μg), and Gcn4 (±100 ng) and the reaction initiated upon addition of nucleotides (1.6 mM ATP/CTP, 30 μM UTP, 5 μCi [α -^{32}P]-UTP) in 60 mM KOAc, 40 mM Hepes pH 7.6, 2.5 mM $MgSO_4$, 2.5 mM DTT, 3.34% wt/vol PEG 8 K, 24 mM creatine phosphate, 1.8 mg/mL creatine kinase, and 20 U RNaseOUT. Reactions were performed at 30 °C for 40 min before stopping in buffer containing RNase T1 (20 U), followed by proteinase K digestion, ethanol precipitation of RNA, and analysis with 6% denaturing PAGE and phsphoimaging techniques.

Selemethionine Incorporation in Mediator Head Module. A 5-mL culture of the CB010 MED8-TAP ΔSIN4 strain was grown to 6.0 A_{600} in a rich synthetic complete media [0.09 mg/mL each of adenine sulfate, uracil, L-tryptophan, L-histidine-HCl, L-arginine-HCl, L-tyrosine, L-leucine, L-isoleucine and L-lysine-HCl with 0.3 mg/mL each of L-glutamic acid, L-aspartic acid, L-glutamine, succinic acid, 0.2 mg/mL L-proline and L-alanine, 0.15 mg/mL L-phenylalanine, 0.45 mg/mL L-valine, 0.6 mg/mL threonine, 1.2 mg/mL L-serine, 0.12 mg/mL L-cysteine, 0.34 mg/mL thiamine, 0.01 mg/mL inositol, 0.145% wt/vol yeast nitrogen base without amino acids (DiFco), 38 mM ammonium sulfate, and 3% wt/vol dextrose] containing 0.1 mg/mL methionine and 100 μg/mL ampicillin. Cells were pelleted, washed repeatedly in sterile H_20, and resuspended in rich synthetic complete media containing 0.1 mg/mL selenomethionine (Fisher Scientific). Cells were amplified to a final volume of 100 L and harvested at 4.6 A_{600} yielding around 850 g dry mass. Mediator Head containing selenomethionine was purified using an identical procedure to the wild-type complex.

Chemical Cross-Linking and LC-MS Analyses. Before cross-linking, the Mediator Head module was dialyzed against three changes of phosphate buffer [150 mM sodium phosphate pH 7.6, 5% (vol/vol) glycerol, 5 mM DTT] to remove primary amines. Approximately 40 μg of Mediator Head module that had been cross-linked with a 1:1 mixture of D_0:D_{12} BS3 (8 mM BS3 on ice for 120 min) was treated with 10 mM TCEP for 20 min at 56 °C, followed by 20 mM iodoacetamide for 1 h at room temperature to reduce and alkylate cysteine residues. The pH was then adjusted to 8.0 with 100 mM ammonium bicarbonate and the sample was digested overnight at 37 °C with side chain modified trypsin (Promega), added at a 1:30 (w:w) ratio. The digest was acidified to 0.3% TFA, solid-phase–extracted using a C_{18} OMIX tip (Agilent), and vacuum dried.

High pH C_{18} chromatography was performed using an AKTA Purifier (GE Healthcare) on an 1.0 × 100-mm column packed with 3 μm, 110 Å Gemini C_{18} resin (Phenomenex). Next, 20 μg of cross-linked, digested Head module was loaded onto the column in 99% buffer A (10 mM ammonium formate, pH 10.1), 1% buffer B [10 mM ammonium formate, 50% (vol/vol) acetonitrile, pH 10.1] at a flow rate of 100 μL/min. Peptides were eluted with a gradient from 1–65% B over 5 mL and collected into 13 fractions, which were dried on a centrifugal evaporator to remove solvent and ammonium formate.

Both fractionated and unfractionated cross-linked samples were analyzed on an LTQ-Orbitrap Velos mass spectrometer (Thermo Scientific) equipped with a Nanoacquity UPLC system (Waters). Peptides were resuspended in 0.1% formic acid and separated at 600 nL/min on a 75 μm × 150 mm BEH130 C_{18} column (Waters). Solvent A was 0.1% formic acid in water and solvent B was 0.1% formic acid in acetonitrile. Peptides were eluted with a gradient of 3–27% B followed by a short wash at 50% B before returning to the initial conditions. The length of the gradient varied from 33 to 153 min, depending on the expected complexity of the fraction. MS spectra were measured in the Orbitrap from 300 to 2,000 *m/z* at 30,000 resolving power. HCD product ions were measured in the Orbitrap analyzer at 7,500 resolving power.

Half of each fraction was measured using data-dependent acquisition of the six most abundant, triply charged or higher ions from each MS scan with a 30-s dynamic exclusion window. The data were then analyzed using in-house scripts to detect precursor ion signals that showed doublet patterns characteristic of a 1:1 mixture of light and heavy cross-linking reagent. Inclusion lists were generated targeting these ions that were separated by 12.0753 Da, and the other half of each sample was then rerun, selecting only the precursors from the inclusion list.

MS Data Analysis. Peak-lists from all MS runs were generated using a combination of PAVA (University of California at San Francisco) (6) and Hardklör (University of Washington) (7). Cross-linked peptides were analyzed with Protein Prospector (University of California at San Francisco) (8, 9). Peak-lists were first searched against the SwissProt database (January 2011, 524,420 entries) to identify contaminating proteins. Cross-link searches were conducted against a database containing the 7× Mediator Head module sequences plus randomized versions of the same sequences. Finally, all putative cross-links were searched against a database containing all of the Mediator subunits as well as all low-level contaminants identified in the first search and randomized versions of these protein sequences (210 entries total). Carbamidomethylation of cysteine was considered as a fixed modification. N-terminal methionine loss and acetylation, N-terminal glutamine conversion to pyroglutamate, oxidation of methionine, and "dead-end" modifiation of lysine by hydrolyzed D_0 or D_{12} BS3 cross-linker were considered as variable modifications. Mass tolerances of 8 ppm for precursors and 20 ppm for product ions were used.

A score threshold for reporting cross-linked peptides was chosen such that all hits to the decoy sequences were excluded (some lower scores accepted after manual validation); this corresponded to a Protein Prospector W Score of 6. Furthermore, precursor ions were checked manually to ensure that the monoisotopic precursor and charge were assigned correctly in the peak-lists and that the isotopic composition of the cross-linker annotated in the search results matched correctly the light or heavy half of the observed isotope distributions. Product ion spectra were inspected to assess whether sufficient backbone fragments were present to positively identify both of the cross-linked peptides as well as the covalently modified residues. When there was sufficient evidence to identify both of the cross-linked peptides but the exact site of modification were ambiguous, all possible sites were reported. Additionally, product ion spectra were annotated as high confidence or medium confidence based on the product ion coverage as well as the extent of unassigned ion signals present in the spectrum.

1. Ranish JA, Lane WS, Hahn S (1992) Isolation of two genes that encode subunits of the yeast transcription factor IIA. *Science* 255:1127–1129.
2. Liu X, Bushnell DA, Wang D, Calero G, Kornberg RD (2010) Structure of an RNA polymerase II-TFIIB complex and the transcription initiation mechanism. *Science* 327: 206–209.
3. Sayre MH, Tschochner H, Kornberg RD (1992) Reconstitution of transcription with five purified initiation factors and RNA polymerase II from *Saccharomyces cerevisiae*. *J Biol Chem* 267:23376–23382.
4. Takagi Y, Kornberg RD (2006) Mediator as a general transcription factor. *J Biol Chem* 281:80–89.
5. Kong SE, Svejstrup JQ (2002) Incision of a 1,3-intrastrand d(GpTpG)-cisplatin adduct by nucleotide excision repair proteins from yeast. *DNA Repair (Amst)* 1: 731–741.
6. Guan S, Price JC, Prusiner SB, Ghaemmaghami S, Burlingame AL (2011) A data processing pipeline for mammalian proteome dynamics studies using stable isotope metabolic labeling. *Mol Cell Proteomics* 10(12): M111.010728.

7. Hoopmann MR, Finney GL, MacCoss MJ (2007) High-speed data reduction, feature detection, and MS/MS spectrum quality assessment of shotgun proteomics data sets using high-resolution mass spectrometry. *Anal Chem* 79:5620–5632.
8. Chu F, Baker PR, Burlingame AL, Chalkley RJ (2010) Finding chimeras: A bioinformatics strategy for identification of cross-linked peptides. *Mol Cell Proteomics* 9:25–31.
9. Trnka MJ, Burlingame AL (2010) Topographic studies of the GroEL-GroES chaperonin complex by chemical cross-linking using diformyl ethynylbenzene: The power of high resolution electron transfer dissociation for determination of both peptide sequences and their attachment sites. *Mol Cell Proteomics* 9:2306–2317.

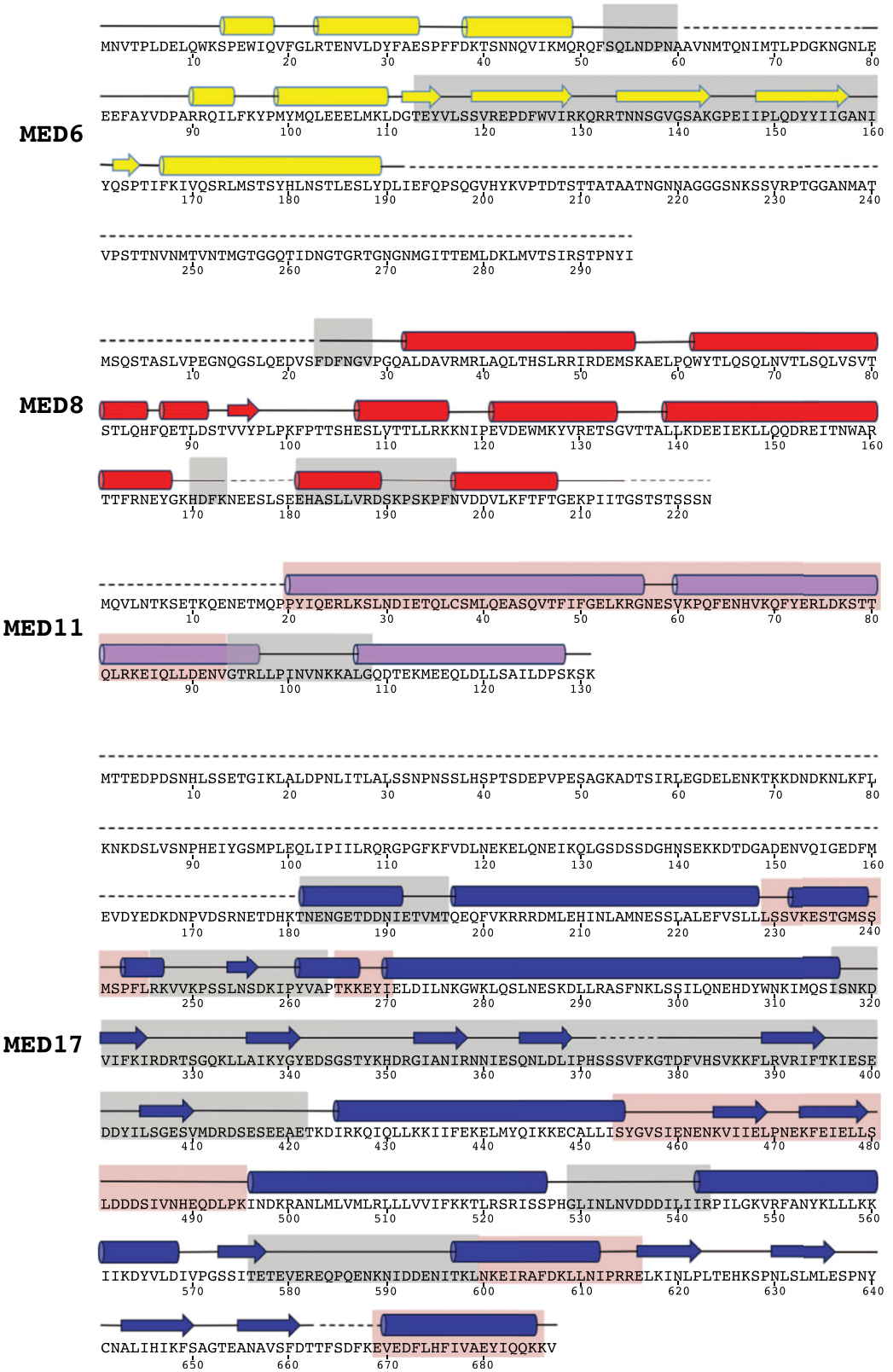

Fig. S1. (Continued)

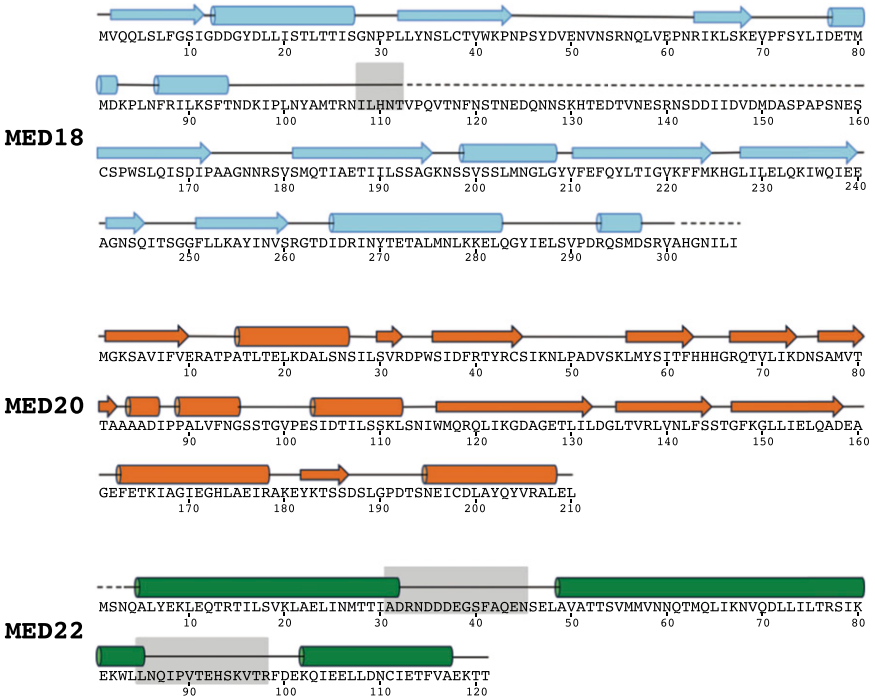

Fig. S1. Graphical representation of secondary structure elements and model revisions for Mediator Head module subunits. Secondary structure is shown above the protein sequence for each Head module subunit: helical regions are represented with cylinders, sheets with arrows, and loops with continuous lines. Regions of gray shading represent sections of new model built in currently unmodelled sequence. Pink shading represents models sections where the atomic coordinates vary significantly from corresponding regions of the existing model [Protein Database Identification (PID): 3RJ1].

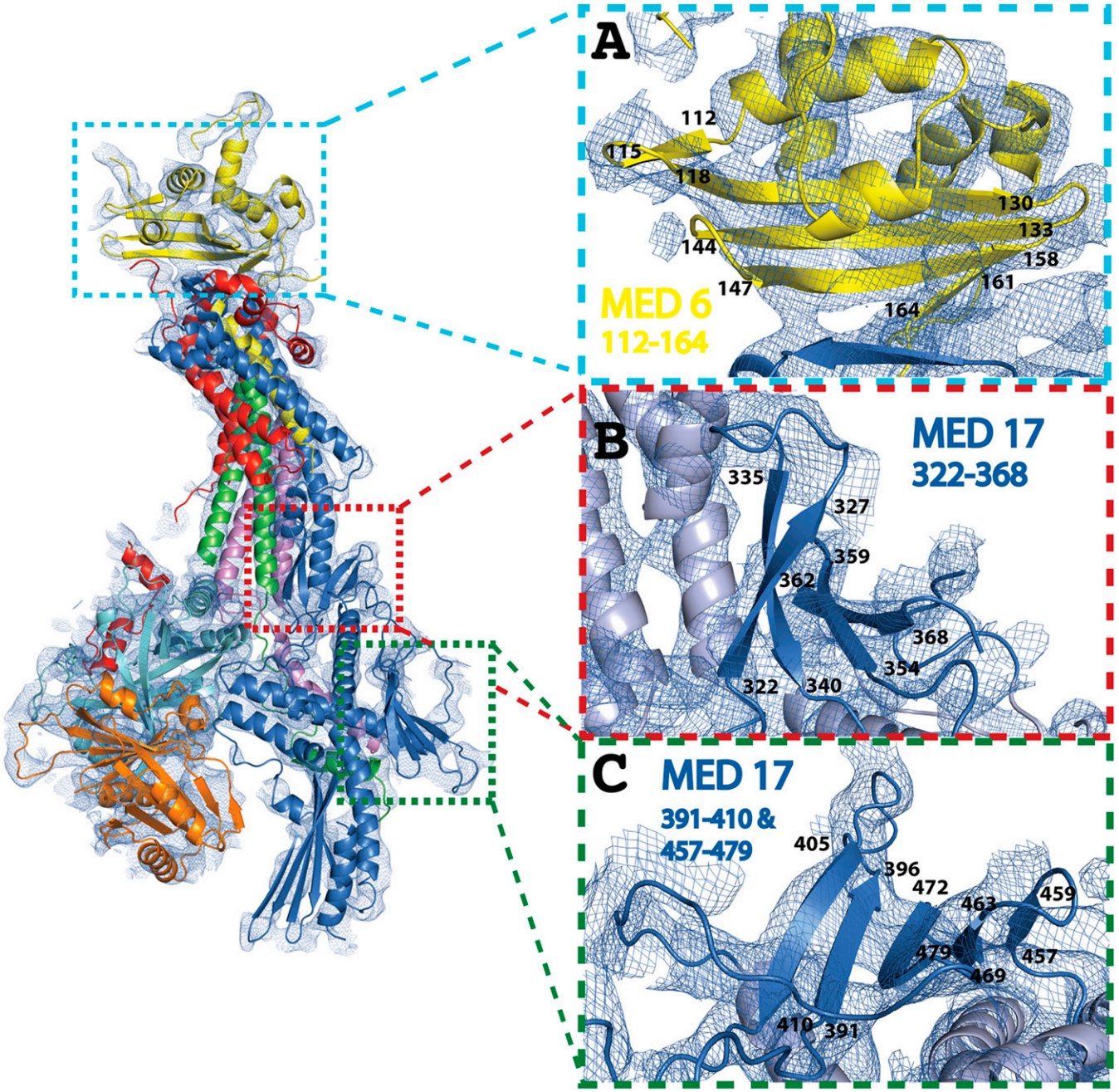

Fig. S2. Modeling new β-sheet regions. The strong phasing power of the multiple isomorphous replacement with anomalous scattering (MIRAS) data enabled three extra regions of β-sheet to be resolved and modeled. (*A*) Residues Med6 112–164 (blue boundary) form a five-strand antiparallel β-sheet. Strand orientation was deduced from the position of entry and exit density and sequence register was guided by secondary structure prediction using the JPRED server. For clarity, the Med8 sequence was omitted. (*B*) Residues Med17 322–368 (red boundary) form a sheet region within the Joint domain comprising two pairs of antiparallel strands arranged roughly perpendicular to one another but coupled through a short stretch of antiparallel sheet. For clarity, sections of Med18 and Med11 were omitted and nonsheet sequence colored light blue. (*C*) Sequences from disparate sections of the Med17 C terminus (residues 391–410 and 457–479; green boundary) associate in a five-strand antiparallel β-sheet. As with *A*, the detailed organization of the sheet was deduced from entry/exit and loop density combined with secondary structure prediction. For clarity, sections of Med11 and Med22 were omitted and nonsheet sequence colored light blue. In each panel the model is overlaid with map density from experimental MIRAS phasing contoured at 1.0 σ (blue mesh).

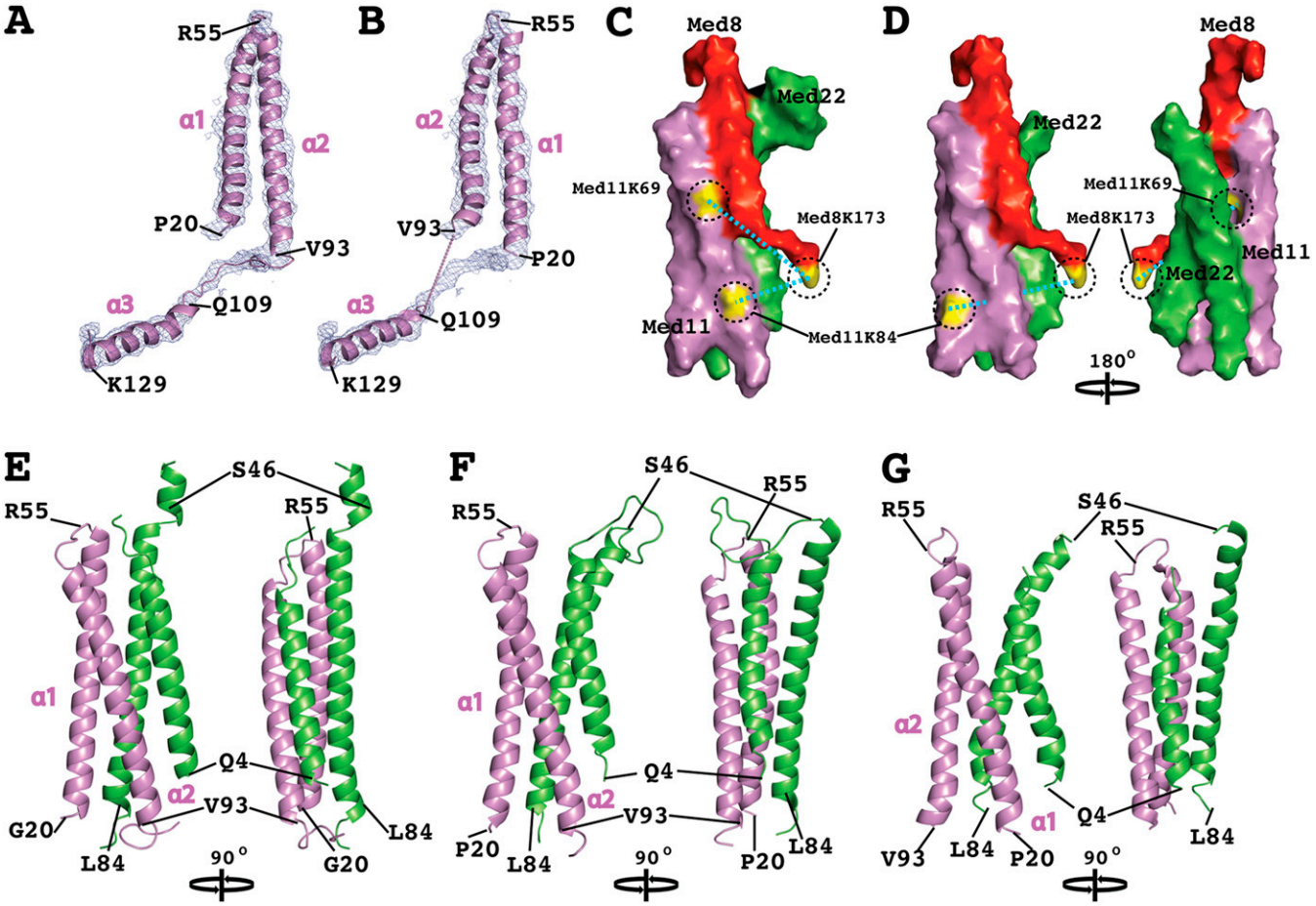

Fig. S3. Revision of Med11 N-terminal helices. (*A*) Revised model of Med11 with N-terminal helical directionality (α1–α2) opposite to that proposed in existing model (PID: 3RJ1). Ribbon is overlaid with weighted map ($2F_0$-F_C; blue mesh; 1.5 σ contouring) showing clear density for the linker between the C terminus of helix 2 (V93) and the N terminus of helix 3 (Q109). (*B*) Ribbon model of Med11 from 3RJ1 with helices aligned to fit into current weighted electron density map. The dashed line connecting helix 2 and helix 3 represents the path of the unmodelled 16-residue linker, which lies outside electron density. (*C*) Cross-linking constraints support the revised Med11 model. LC-MS/MS analysis of BS3–cross-linked Mediator Head module identified two Med8K173 cross-links; one with Med11K84 and another with Med11K69. These cross-links are shown as dashed lines on a surface representation of the Med11-Med22-Med8 helical bundle region (Med11 20–93; Med22 4–86; Med8 136–173). Cross-linked residues are colored yellow. (*D*) Two views of a surface representation of the Med11-22-8 bundle with Med11 and Med22 sequences derived from 3RJ1. Views are related by 180° rotation around the vertical axis. Equivalent cross-links from *C* are displayed. Breaks in the dashed line represent steric obstructions in the cross-linking path. (*E*) Rotated ribbon model of the Med11-Med22 N-terminal helical bundle determined at high resolution (PID: 3R84). (*F*) The equivalent model section as *E* from the present study shows consistency in overall organization and sequence directionality with the high-resolution model. (*G*) Model of equivalent sequence from 3RJ1 shows reversal in directionality of Med11 N-terminal helices in respect to high-resolution model.

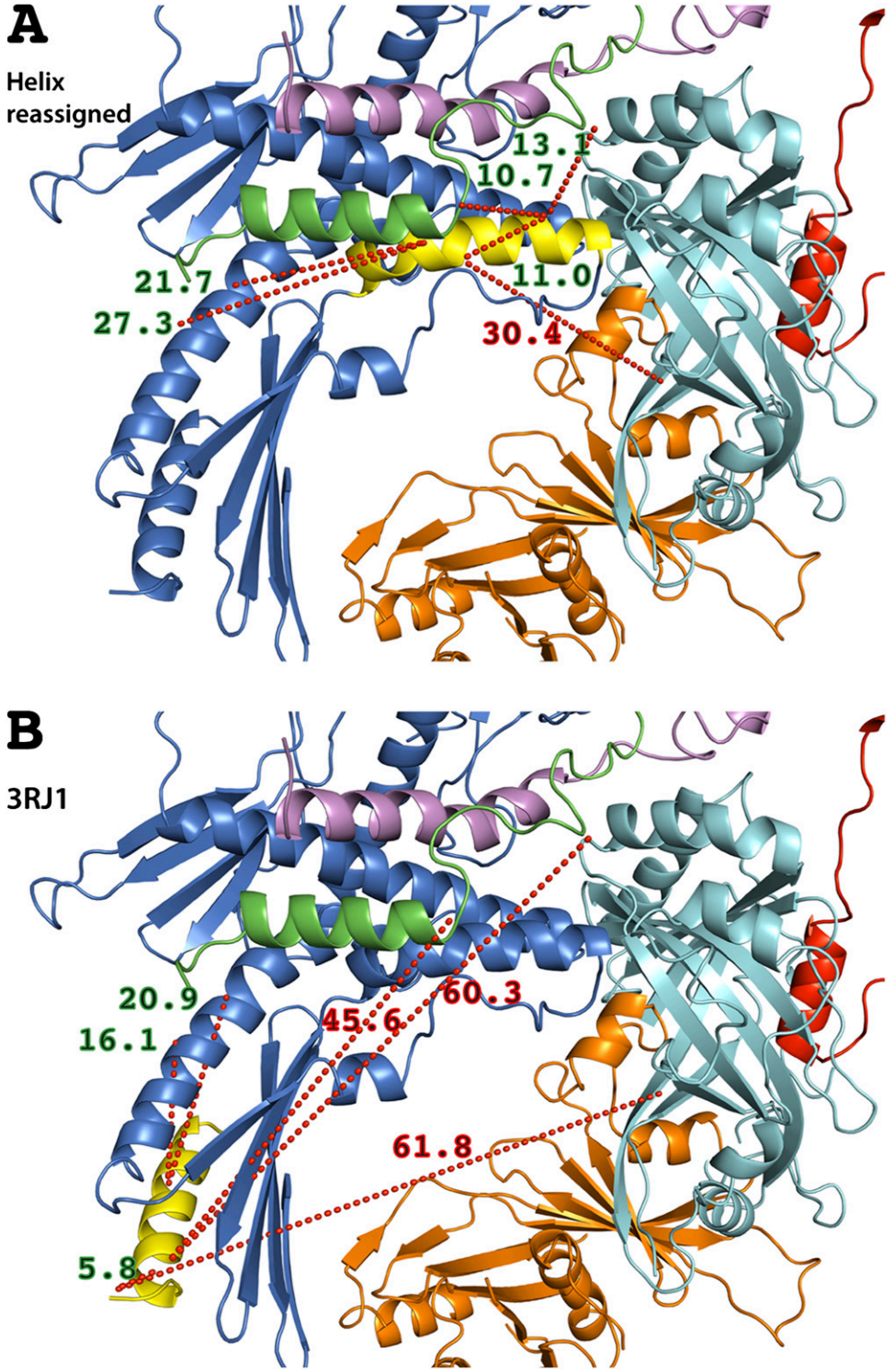

Fig. S4. Revised sequence assignment in Med17 C-terminal domain (Fixed Jaw). LC-MS/MS analysis of BS3–cross-linked Mediator Head module supports reassignment of the Med17 C-terminal helices 597–611 and 670–685 and surrounding sequence. Cβ cross-link distances less than the standard 30 Å cutoff are labeled in green and those greater than 30 Å are labeled red. (*A*) Cross-linking pattern generated between Med17 K589, K601, and K608 and surrounding lysines resulting from the revised assignment of helix 597–611 (yellow). Cross-links are shown with dashed red lines and the modeled Cβ cross-link distances are displayed alongside. Mediator subunits are individually colored: Med8 (red), Med11 (violet), Med17 (blue), Med22 (green). Cross-links displayed: Med17 K589-Med18K68, Med17K589-Med17K601, Med17K601-Med22K95, Med17K601-Med22K105, Med17K608-Med17K555, and Med17K608-Med17K559. (*B*) Representative cross-linking pattern for the cross-links described in *A*, resulting from the 3RJ1 assignment of helix 597–611 (yellow). Cross-links representative of the 3RJ1 assignment were generated using current model coordinates by mapping the 3RJ1 assignment of helix 597–611 to the positionally equivalent residues 670–685 in the present model (Med17K601 equivalent to Med17K685 and Med17K608 equivalent to Med17V678). Because Med17K589 was previously unmodelled, cross-links involving this residue were represented by linking with the closest possible 3RJ1 modeled residue (Med17N600 equivalent to current Med17K686). Subunits and cross-links colored and labeled as in *A*.

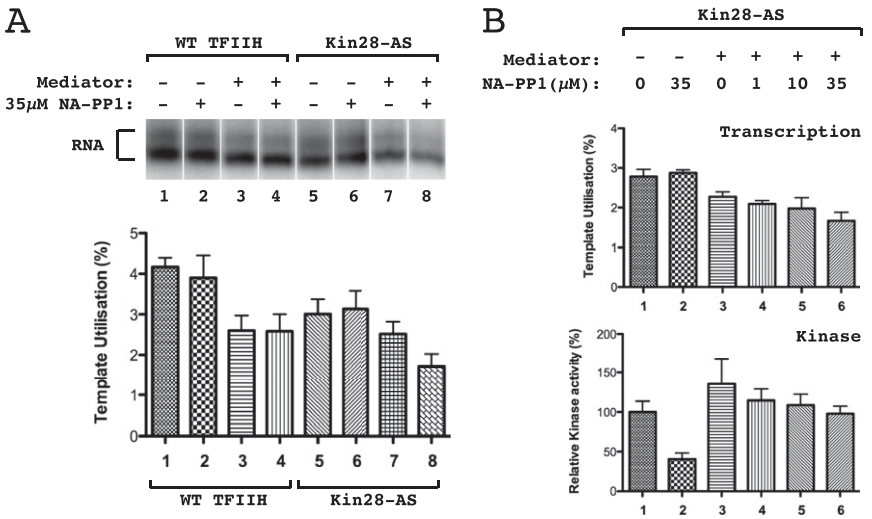

Fig. S5. Mediator-dependence of transcriptional response to CTD kinase inhibitor. (*A*) A 208-bp linear *HIS4* promoter DNA fragment was transcribed with purified proteins and α-^{32}P-UTP, followed by gel electrophoresis and phosphorimage analysis, as described above. Reactions were performed with wild-type or inhibitor-sensitive TFIIH (Kin28-AS), with and without Mediator, and with and without Kin28-AS inhibitor NA-PP1, as indicated. (*B*) The inclusion of γ-^{32}P -ATP in the transcription reaction allowed for the quantification of both the transcription and CTD kinase activity of each sample. Reactions were performed with Kin28-AS, with and without Mediator and the indicated levels of NA-PP1.

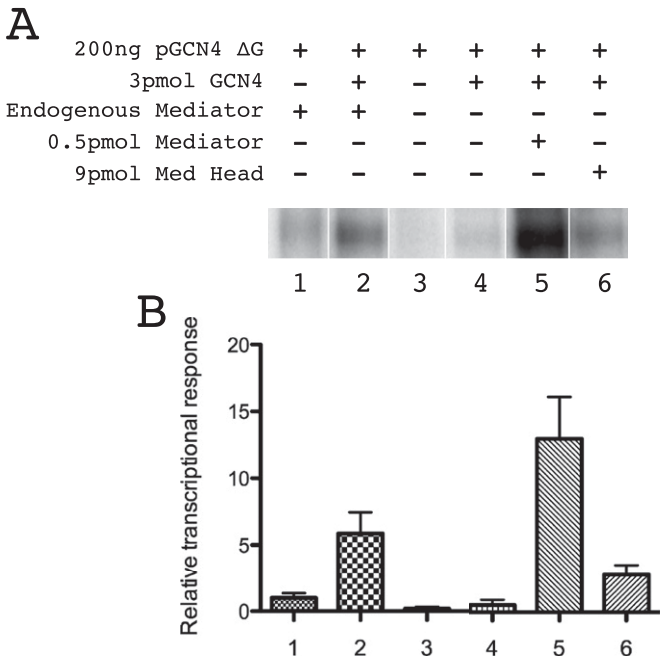

Fig. S6. Purified Mediator complexes recover activity in depleted extract. (*A*) In vitro transcription from WCE was performed from a plasmid-based promoter template (pGCN4 ΔG) carrying a GCN4 UAS and downstream Gless cassette, as described above and detected by incorporation of ^{32}P αUTP followed by denaturing PAGE and phosphorimaging. Reactions were performed using extract in which endogenous Mediator was either present or completely depleted by affinity capture. Transcription responses were analyzed with and without supplementation of purified GCN4, Mediator, and Mediator Head module. (*B*) Transcriptional levels in *A* were quantified from at least three independent measurements and normalized against the signal from unmodified extract.

Table S1. Data collection, phasing and refinement statistics for MIRAS (Ta_6Br_{12} & Au) structures

Data collection and statistics	Native	Ta_6Br_{12} MAD			Au SAD
Data collection					
Space group	$P3_221$		$P3_221$		$P3_221$
Cell dimensions					
a, *b*, *c* (Å)	142.0, 142.0, 305.3		140.8, 140.8, 307.4		141.9, 141.9, 306.1
α, β, γ (°)	90.0, 90.0, 120.0		90.0, 90.0, 120.0		90.0, 90.0, 120.0
		Peak	Inflection	Remote	Peak
Wavelength	0.98 Å	1.1134 Å	1.1137 Å	1.0748 Å	1.0377 Å
Resolution (Å)	52.6–4.2 (4.43–4.2)*	45.0–5.0 (5.27–5.0)	45.0–5.0 (5.27–5.0)	45.0–4.5 (4.74–4.5)	55.0–5.5 (5.84–5.5)
R_{sym} or R_{merge}[†]	0.08 (0.77)	0.08 (0.77)	0.08 (0.66)	0.08 (0.66)	0.11 (0.87)
$I/\sigma I$	11.5 (2.0)	15.7 (3.9)	15.3 (4.2)	15.9 (4.4)	16.1 (3.3)
Completeness (%)	99.4 (97.7)	99.8 (100)	99.9 (100)	99.8 (100)	99.9 (100)
Redundancy	5.3 (5.0)	14.5 (14.8)	14.0 (14.4)	14.1 (14.4)	13.1 (13.4)
Phasing					
Phasing power isomorphous		2.66 (1.068)	2.38 (0.949)	2.22 (0.31)	0.423 (0.32)
Phasing power anomalous		2.99 (0.687)	2.38 (0.526)	2.16 (0.217)	0.21 (0.095)
FOMacen (combined)		—	—	—	0.72 (0.13)
FOMcen (combined)					0.62 (0.14)
Refinement					
Resolution (Å)	45.0–4.2				
No. reflections	25,254				
R_{work}[‡]/R_{free}[§]	29.0/35.7				
No. atoms					
Protein	12,350				
Ligand/ion					
Water					
B-factors	219.2				
Protein					
Ligand/ion					
Water					
R.m.s deviations					
Bond lengths (Å)	0.011				
Bond angles (°)	1.616				
PDB accession	4GWP				

*Values in parentheses are from the highest resolution shell.

[†]$R_{merge} = \Sigma|I-\langle I\rangle|/\Sigma\langle I\rangle$.

[‡]$R_{work} = \Sigma||Fo|-|Fc||/\Sigma|Fo|$.

[§]$R_{free} = \Sigma T||Fo|-|Fc||/\Sigma T|Fo|$, where T is a test data set of 5% of the total reflections randomly chosen and set aside before refinement.

Table S2. Data collection and refinement statistics (CTD peptide soaks)

Data collection and refinement	5× CTD peptide soak	2× CTD peptide soak
Data collection		
Space group	$P3_221$	$P3_221$
Cell dimensions		
a, *b*, *c* (Å)	142.5, 142.5, 305.6	142.0, 142.0, 305.2
α, β, γ (°)	90.0, 90.0, 120.0	90.0, 90.0, 120.0
Resolution (Å)	39.8–4.5 (4.7–4.5)*	44.5–4.3 (4.5–4.3)
R_{sym} or R_{merge}[†]	0.1 (0.68)	0.06 (0.59)
$I/\sigma I$	17.7 (4.5)	9.0 (1.9)
Completeness (%)	99.8 (100.0)	99.6 (99.9)
Redundancy	14.4 (14.7)	2.7 (2.8)
Refinement		
Resolution (Å)	45.0–4.5	
No. reflections	20,920	
R_{work}[‡]/R_{free}[§]	28.6/34.5	
No. atoms		
Protein	12,532	
Ligand/ion		
Water		
B-factors		
Protein	258.7	
Ligand/ion		
Water		
R.m.s deviations		
Bond lengths (Å)	0.01	
Bond angles (°)	1.56	
PDB accession	4GWQ	

*Values in parentheses are from the highest resolution shell.

[†]$R_{merge} = \Sigma|I-\langle I\rangle|/\Sigma\langle I\rangle$.

[‡]$R_{work} = \Sigma||Fo|-|Fc||/\Sigma|Fo|$.

[§]$R_{free} = \Sigma T||Fo|-|Fc||/\Sigma T|Fo|$, where T is a test data set of 5% of the total reflections randomly chosen and set aside before refinement.

Table S3. Data collection, phasing and refinement statistics for selenomethionine (SeMet) SAD

Data collection and refinement	SeMet SAD
Data collection	
Space group	$P3_221$
Cell dimensions	
a, *b*, *c* (Å)	139.4, 139.4, 305.3
α, β, γ (°)	90.0, 90.0, 120.0
	Peak
Wavelength	0.98 Å
Resolution (Å)	120.7–5.0 (5.25–5.0)*
R_{sym} or R_{merge}[†]	0.12 (0.75)
$I/\sigma I$	11.0 (2.4)
Completeness (%)	96.3 (93.4)
Redundancy	8.5 (7.8)
Refinement	
Resolution (Å)	
No. reflections	
R_{work}[‡]/R_{free}[§]	
No. atoms	
Protein	
Ligand/ion	
Water	
B-factors	
Protein	
Ligand/ion	
Water	
R.m.s deviations	
Bond lengths (Å)	
Bond angles (°)	

*Values in parentheses are from the highest resolution shell.

[†]$R_{merge} = \Sigma|I-\langle I\rangle|/\Sigma\langle I\rangle$.

[‡]$R_{work} = \Sigma||Fo|-|Fc||/\Sigma|Fo|$.

[§]$R_{free} = \Sigma T||Fo|-|Fc||/\Sigma T|Fo|$, where T is a test data set of 5% of the total reflections randomly chosen and set aside before refinement.

Table S4. Summary of Mediator Head BS3 cross-links

m/z	*z*	ppm	BS3 Isotope	Alt. isotope obs.	Peptide 1	Peptide 2	W Score	Confidence	Res1	Res2	Res1-alt	Res2-alt	Cβ distance (Å)
803.942	6	7.5	Light	—	K*VVKPSSLNSDKIPYVAPTKK	TGNGNMGITTEMLDK*LMVTSIR	36.4	High	247.Med17	282.Med6	—	—	282.Med6 unmodelled
845.203	4	2.1	Light	—	K*EYIELDILNK	ETSGVTTALLK*DEEIEK	22.6	High	267.Med17	141.Med8	—	—	17.7
899.017	4	4.5	Heavy	+	IMQSISNK*DVIFK	WLLNQIPVTEHSK*VTR	21.7	High	319.Med17	95.Med22	—	—	17.5
747.694	4	7.2	Light	—	IMQSISNK*DVIFKIR	TSGQK*LLAIK	12.7	Medium	319.Med17	333.Med17	—	—	31.0
696.097	3	5.7	Light	+	DVIFK*IR	TSGQK*LLAIK	22.1	High	324.Med17	333.Med17	—	—	14.4
745.467	3	0.3	Light	+	TSGQK*LLAIK	LLPINVNK*K	20.8	High	333.Med17	104.Med11	—	—	19.2
939.847	3	−3.1	Light	+	TSGQK*LLAIK	Acetyl-SNQALYEK*LEQTR	12.6	High	333.Med17	9.Med22	—	—	20.1
714.418	4	−6.7	Heavy	+	TSGQK*LLAIK	K*ELQGYIELSVPDR	17.4	High	333.Med17	280.Med18	—	—	22.1
439.007	4	−0.2	Light	—	K*FLR	ELMYQIK*K	12.0	High	387.Med17	446.Med17	—	—	14.9
447.035	4	−3.5	Light	—	K*QIQLLK	K*IIFEK	27.8	High	427.Med17	434.Med17	—	—	10.6
700.631	4	7.9	Light	+	INDK*R	MEEQLDLLSAILDPSK*SK	1.6	Medium	499.Med17	129.Med11	—	—	12.1
1012.512	3	−1.0	Light	—	INDK*R	QIEELLDNC(Cam)IETFVAEK*TT	6.8	Medium	499.Med17	119.Med22	—	—	16.7
623.091	7	7.4	Light	—	ISSPHGLINLNVDDDILIIRPILGK*VR	FANYK*LLLKK	12.3	High	548.Med17	555.Med17	—	—	11.4
854.516	3	4.2	Light	—	FANYK*LLLKK	AFDK*LLNIPR	52.6	High	555.Med17	608.Med17	—	—	21.7
878.732	4	0.6	Heavy	—	FANYK*LLLK	QIEELLDNC(Cam)IETFVAEK*TT	12.3	High	555.Med17	119.Med22	—	—	6.6
807.712	4	−3.6	Light	—	LLLK*K	IIK*DYVLDIVPGSSITETEVER	8.7	Medium	559.Med17	563.Med17	—	—	7.2
858.533	3	−5.1	Heavy	+	FANYK*LLLK*K	AFDK*LLNIPR	20.1	High	559.Med17	608.Med17	555.Med17	608.Med17	27.3
1000.563	3	2.8	heavy	—	LLLK*K	Q(Gln->pyro-Glu)IEELLDNC(Cam) IETFVAEK*TT	0.8	Medium	559.Med17	119.Med22	—	—	7.4
942.143	3	−6.6	Light	—	EQPQENK*NIDDENITK	LNK*EIR	19.9	High	589.Med17	601.Med17	—	—	11
1014.118	5	4.3	Light	—	EQPQENK*NIDDENITK	IK*LSK*EVPFSYLIDETMMDKPLNFR	39.3	High	589.Med17	68.Med18	589.Med17	65.Med18	30.4
1207.103	4	6.9	Light	+	EQPQENK*NIDDENITK	LSK*EVPFSYLIDETMMDKPLNFR	31.6	High	589.Med17	68.Med18	—	—	30.4
569.341	5	2.7	Heavy	+	LNK*EIR	WLLNQIPVTEHSK*VTR	7.9	Medium	601.Med17	95.Med22	—	—	13.1
1160.585	3	−6.2	Light	—	LNK*EIR	FDEK*QIEELLDNC(Cam)IETFVAEK	15.2	High	601.Med17	102.Med22	—	—	12.8
833.135	3	−7.5	Heavy	—	*-MQVLNTK	K*EIQLLDENVGTR	14.8	High	1.Med11	84.Med11	—	—	1.Med11 unmodelled
940.295	5	−1.1	Light	—	LK*SLNDIETQLC(Cam) SMLQEASQVTFIFGELKR	LDK*STTQLR	22.2	High	27.Med11	77.Med11	—	—	16.3
1033.355	5	−0.9	Heavy	+	LK*SLNDIETQLC(Cam) SMLQEASQVTFIFGELKR	K*EIQLLDENVGTR	48.1	High	27.Med11	84.Med11	—	—	14.6
730.555	6	−5.7	Heavy	—	GNESVK*PQFENHVK	ETSGVTTALLK*DEEIEK*LLQQDR	8.8	Medium	61.Med11	141.Med8	61.Med11	147.Med8	24.8
738.982	5	−5.4	Light	—	RGNESVKPQFENHVK*QFYER	LDK*STTQLR	32.8	High	69.Med11	77.Med11	—	—	12.2
760.384	7	1.8	Heavy	—	GNESVK*PQFENHVK*QFYER	NEYGK*HDFK*NEESLSEEHASLLVR	8.5	Medium	69.Med11	173.Med8	61.Med11	169.Med8	27.5
905.166	3	3.9	Light	—	LDK*STTQLR	K*EIQLLDENVGTR	40.2	High	77.Med11	84.Med11	—	—	10.1
674.518	6	−5.4	Heavy	—	LDK*STTQLR	NEYGK*HDFK*NEESLSEEHASLLVR	15.0	High	77.Med11	169.Med8	77.Med11	173.Med8	10.8
781.616	5	0.8	Heavy	—	K*EIQLLDENVGTR	HDFK*NEESLSEEHASLLVR	9.6	Medium	84.Med11	173.Med8	—	—	16.5
981.047	4	4.1	Heavy	+	Acetyl-SNQALYEK*LEQTR	SIK*EK*WLLNQIPVTEHSK	42.5	High	9.Med22	80.Med22	9.Med22	82.Med22	12.8
814.018	5	5.4	Light	—	HDFK*NEESLSEEHASLLVR	DSK*PSKPFNVDDVLK	2.0	Medium	173.Med8	191.Med8	—	—	15.7
944.705	5	6.2	Heavy	—	EVPFSYLIDETMMDK*PLNFR	ILK*SFTNDKIPLNYAMTR	27.2	High	83.Med18	91.Med18	—	—	11.9
1092.048	4	−7.4	Heavy	—	EVPFSYLIDETMMDK*PLNFR	SFTNDK*IPLNYAMTR	26.9	High	83.Med18	97.Med18	—	—	20
1125.572	3	3.1	Light	—	TENVLDYFAESPFFDK*TSNNQVIK	K*QR	7.0	Medium	39.Med6	130.Med6	—	—	25.3

Key to Modification Annotation: *, Intermolecular cross-linking by BS3 at lysine or protein N terminus; Acetyl, N-terminal acetylation; Cam, Carbamidomethylation of cysteine by iodoacetamide; Cβ distance, Distance between lysine β carbons in refined apo-Mediator Head model (Poly Ala); Ox, Methionine oxidation; Res1-alt, peptide 1 alternative given in the case of ambiguity in the lysine involved in cross-linking; Res2-alt, peptide 2 alternative given in the case of ambiguity in the lysine involved in cross-linking; Alt. isotope obs., a plus sign denotes the observation of both light and heavy cross-linker isotopes whereas a minus sign denotes the observation of a single isotope.